H.M.Salem et al. / ICEHM2000, Cairo University, Egypt, September, 2000, page 586- 598

Minerals Reconnaissance at Saint Catherine Area, Southern Central Sinai, Egypt and their Environmental Impacts on Human Health

Hanaa M. Salem, A. A. ElFouly
Geology Department, Faculty of Sciences, Cairo University, Egypt
Center for Environmental Hazards Mitigation, Cairo University, Egypt
E-mail:HanaaSalem@orex.org; afouly@orex.org

Abstract

Little detailed work on the economic geology of the Precambrian rocks of the Sinai Peninsula has been undertaken. Surveys of the area do indicate the location of numerous veins which were mined in Pharonic to Roman times for copper and/or gold mineralization. In the St. Catherine area, El-Ghawaby et al., (1989) suggested that porphyry copper-style mineralization was present. Remote sensing analysis was carried out to delineate lineaments associated with hydrothermal alteration zones as well as to predict favorable sites for investigations. Field investigations were intended to visit some of the mineral localities in the St. Catherine area to evaluate the style of mineralization and compare and contrast it with better-known systems from other portions of the world.

Introduction

The study of mineral occurrence in the Saint Catherine area, southern central Sinai, Egypt (Figure 1a & 1b) was undertaken to evaluate the potentiality for base and precious metal deposits in the area. Research and fieldwork took place during early April and early July, 2000. Three prospects were visited for evaluation and samples were collected and prepared for petrographic analysis.

Regional Geology

The Sinai Peninsula forms a portion of the Arabo-Nubian Shield and occupies a wedge-shaped block at the north end of the East African Rift system, bound by the Gulf of Aqaba to the southeast and the Gulf of Suez to the southwest. Four distinct phases of evolution for Sinai has been recognized beginning approximately from 1000 Ma (Bentor, 1985) as follows:
Phase (I) is characterized by the emplacement of oceanic tholeiites, mainly pillow basalts, and their plutonic equivalents. These rocks comprise an ophiolite sequence which is tectonically transported and strongly disrupted. Phase (II) (~ 950-650 Ma) is dominated by andesitic volcanism and quartz-dioritic intrusions of island arc affinity.
Phase (III) (~ 640-590 Ma) involved the cratonization of the Arabo-Nubian massif through emplacement of voluminous felsic calc-alkaline plutons and suturing of the massif of the African Craton. Phase (IV) (~ 590-550 Ma) producer per-alkaline, high-level granites and rhyolites (Katharine Province); it affects the entire Arabo-Nubian Shield and all of North and Saharan Africa.

The last 100 million years of this sequence is the portion of interest in and around St. Catherine. Granitic stocks of varying composition outcrop throughout the region, exhibiting little or no deformation. Late-stage pegmatitic dykes and basaltic dykes, interpreted to be much younger, crosscut the entire Precambrian package. These

late dykes are oriented approximately north-south, sub-parallel to Gulf of Aqaba of the East African Rift.

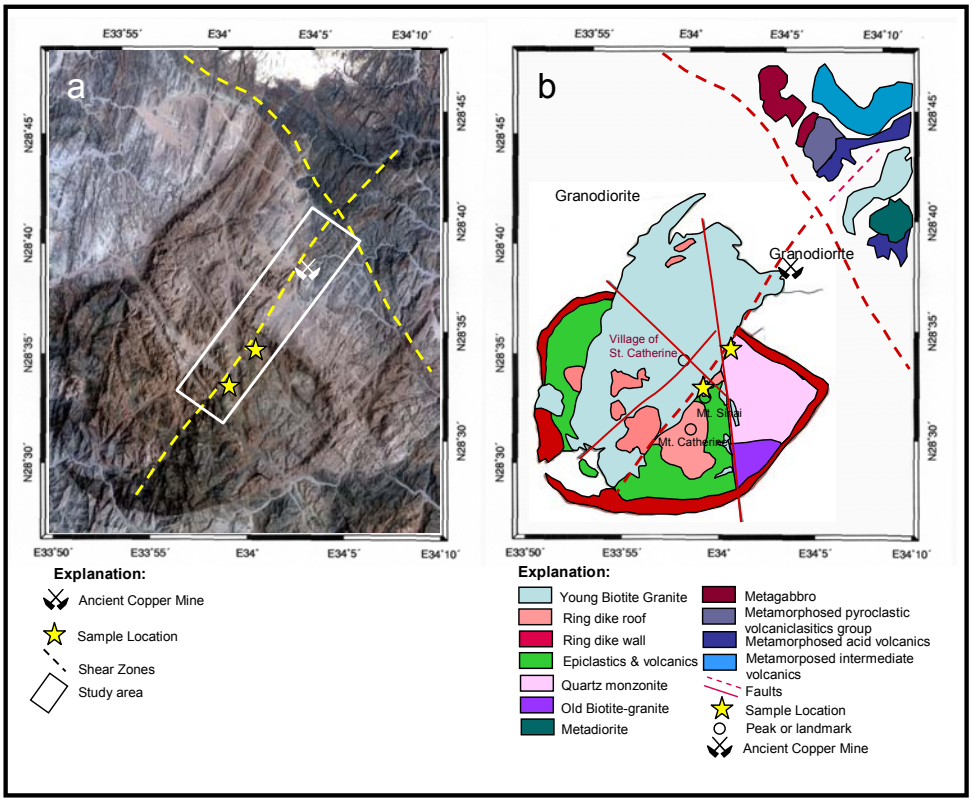

Fig.1. (a) LANDSAT TM image of Saint Catherine Area (Blue: Band 1, Green: Band 2 and Red: Band 3). (b) Geologic map of the Saint Catherine area, Southern Sinai. (modified after El-Masry, et al., 1992).

Base and Precious metal Deposits Investigation at St. Catherine area

Remote sensing study

The use of remote sensing techniques in reconnaissance survey was verified to be a very useful tool for mineral exploration. The purpose of using this technique in this study is to minimize the exploration effort and time in this harsh terrain. The spectral and textural information in LANDSAT-5 TM images of Saint Catherine area were used in this study.

To explore for previously unknown economic mineral deposits we must understand the features by which the deposits are recognized and the methods by which such deposits are detected. In the study area, we were exploring for mineralization related to hydrothermal systems. The exploration model is inspired from the formation of the ore materials. Ore bodies marked by alteration zones are valuable indicators of possible deposits. Alteration minerals commonly occur in distinct sequences, or zones of hydrothermal alteration, relative to the ore body.

Remote sensing relies on recognizing two components for the hydrothermal systems: (a) alunite and clay minerals; and (b) iron mineral associations. Argillic alterations were mainly recognized by using 5/7 ratio image bands, and for hydrothermal iron-alteration by 3/1 ratio image bands. The Density of lineament intersection method

was used to optimize exploration in the studied area associated with alteration zones (El-Fouly, 1992 and El-Fouly et al., 1992). These planes of weakness may provide high-permeability channels for ascent of deeply derived magmas and mineralized fluids.

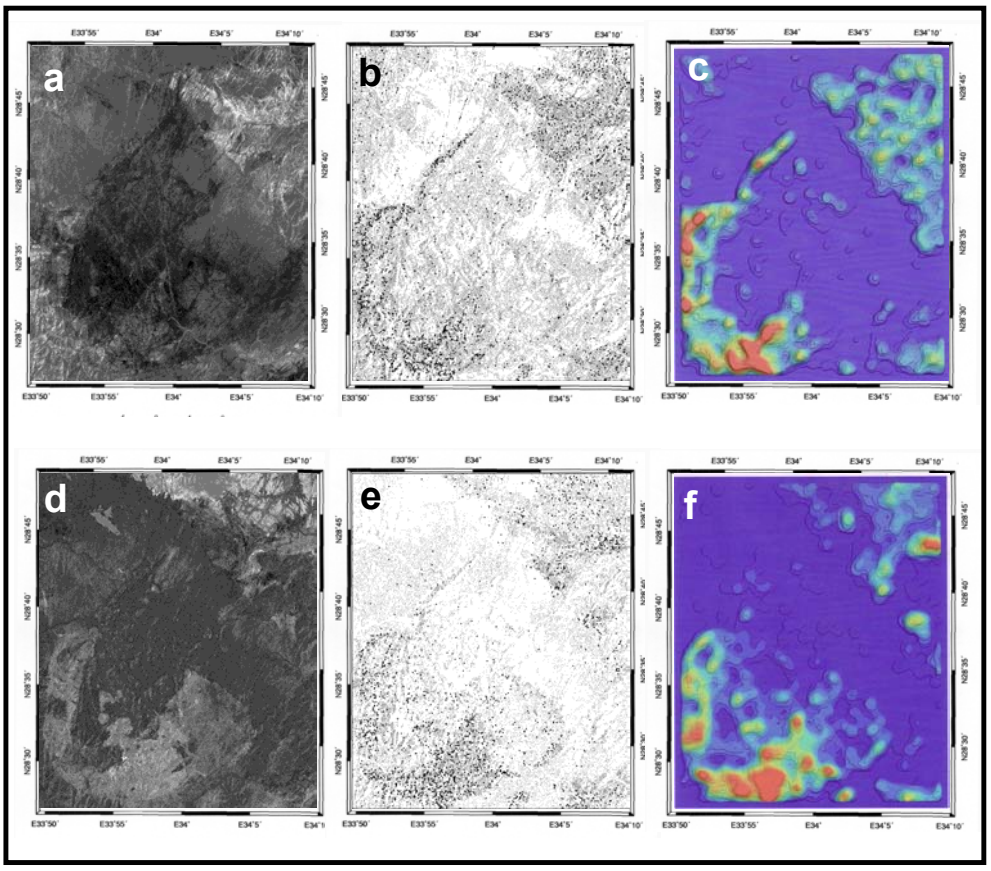

Fig.2. Processing sequence at Saint Catherine area, Southern Sinai. (a) Image of TM 3/1 band ratios shows iron enrichments distribution in the high intensity light gray areas, (b) extracted lineaments (lines) and points of their intersection (dark points) from TM 3/1 band ratios, (c) calculated density of lineaments intersection from TM 3/1 band ratios, (d) image of TM 5/7 band ratios shows hydrothermal alterations distribution in the high intensity light gray areas, (e) extracted lineaments (lines) and points of intersection (dark points) from TM 5/7 band ratios, (f) calculated density of lineaments intersection from TM 5/7 band ratios.

Method and Result

The enrichment of iron and hydrothermal alterations along shear zones in the studied area help to delineate the favorable sites for hydrothermal mineralization. The band ratios of LANDSAT TM bands 5/7 and 3/1 were used to enhance the spectral reflectance of the hydrothermal alteration and iron enrichment respectively (Crippen, 1988). These minerals can be used as good indicator for the hydrothermal fluid effects along fractures during the events of mineralization.

The favorability map was generated for hydrothermal exploration in the studied area by the rationing calculation for 5/7 and 3/1 LANDSTAT-5 TM where shown in figures (2a) & (2d). The intensity in these figures reflects the presence and absence of the hydrothermal alteration and iron enrichments. The delineation of lineaments at Saint

Catherine area using the lineament logic operator was shown in figures (2b) & (2e), as well as the density of intersection in figures (2c) & (2f). The favourabity map for hydrothermal mineralization was shown in figure (3), which assume that the locations that have high density of lineament intersections may have high favourability due to the presence of conduits that are directly associated with alteration zones.

In figure (2a), the iron enrichments are distributed along the west and southwest part of the caldera wall as well as marked the northeastern part formed by the metavolcanics. In figure (2d), the enhanced spectrum of hydrothermal alterations is outlining and filling the pear-like shape of the caldera as well as the main shear zone was delineated along the NE-SW direction between the intruded young biotite granite and the ring dike.

Figures (2e) and (2b) show the extraction of lineaments from the enhanced spectral reflectance of the hydrothermal alteration and iron enrichment through the band rationing of LANDSAT TM bands 5/7 and 3/1. These figures demonstrate all possible lineaments that are only associated with hydrothermal and iron enriched alteration zones. This operation restricts extracted lineaments to those associated with alteration and iron enrichments. The black points in the figure (2e) and (2b) present the locations of intersected lineaments. Figures (2c) and (2f) show the calculated densities for the points of intersected lineaments extracted in figures (2b) and (2e). The high densities are distributed along the caldera wall, and the NE-SW fault along the southeastern contact of the young biotite granite (Figs. 2c & 2f).

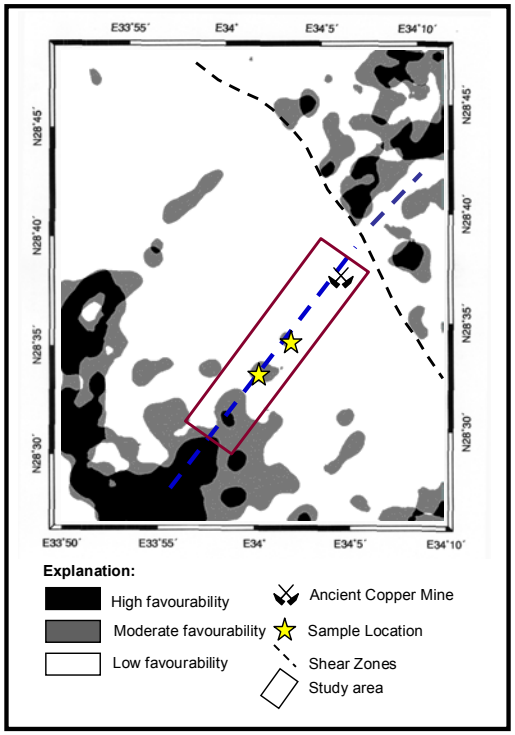

Fig.3. Basic probability assignment map for the predicted copper mineralization sites after the density of lineament Intersection (DLI) extraction.

The black areas in figure (3) show the intersected lineaments associated with both high intensity of hydrothermal alterations and iron enrichments while the gray areas locate the intersected lineaments associated with either hydrothermal alterations or iron enrichments. In general, both black and gray areas are highly considered favourable locations for exploration. The favorability sites are mainly located along the caldera wall especially along the contact between the young biotite granite to the west and to the southwest as well as the contact between the metavolcanics and the old biotite granite at the northeastern corner part of the studied area.

Area of Investigations

Two prospects were selected for examination to evaluate the potentiality for base and precious metal deposits in the study area. These prospects are confined to the hydrothermal alterations along the fault zones that were delineated by the favourability map from remote sensing analysis. And, the abandoned copper mine site was selected as existence copper occurrence in the St. Catherine area. These prospects are:

1- Wadi Umm Qeisum

Wadi Umm Qeisum area is described by El-Ghawaby (1989) as porphyry copper mineralization style. Biotite granite forms the host of the porphyry system. Biotite granite composed of chloritized biotite, epidote, quartz, potassium feldspar with 1-2 cm selvages. Rarely the veins contain trace of pyrite or goethite after pyrite. Veinlet density averages approximately with one veinlet every 3 m.

Biotite granite is intruded by a series of microgranite and aplite dykes and sills. These rocks were observed to have some potassium feldspar "flooding" in the field and rarely contained minor limonite after pyrite. The sulfide content of the rocks never exceeded 1%. This zone of microgranite dykes is cut by rare epidote-quartz veins and quartz veins, some of which contain coarse magnetite or martite after magnetite.

The complex does display weak potassic alteration. This alteration is restricted largely to veins. There has not been a pervasive potassic overprint on the host rocks. Potassic feldspar varies from weak to intense sericitization. This is as a result of hydrothermal alteration; however, there is virtually no quartz-sericite-pyrite veins typical of the late "phyllic" alteration associated with most porphyry systems.
The observed sericitization could be the result of weak porphyry copper style alteration or a weak hydrothermal event which long postdates magmatism as well as a result of intense weathering.

2- Saint Catherine

The rocks in the area surrounding the Monastery of Saint Catherine are dominantly biotite granite (Fig.4a). Late quartz veins, which range from a few centimeters to nearly one meter in width, cut the granite at various orientations. There was no obvious economic mineral association with these veins; however some evidence of prospecting of an unknown age was apparent along the widest veins. Samples were collected from such vein for petrographic analysis. Minor alteration of the surrounding granite had occurred in a narrow selvage immediately adjacent to quartz veins. This alteration is characterized by degradation of felspars to clay and sericite, stained red with iron oxides derived from the weathering or alteration of mafic minerals.

It seems unlikely that any significant economic mineralization was associated with these late quartz veins, given the apparent of sulfide mineral assemblage and hydrothermal textures common in epithermal gold systems.

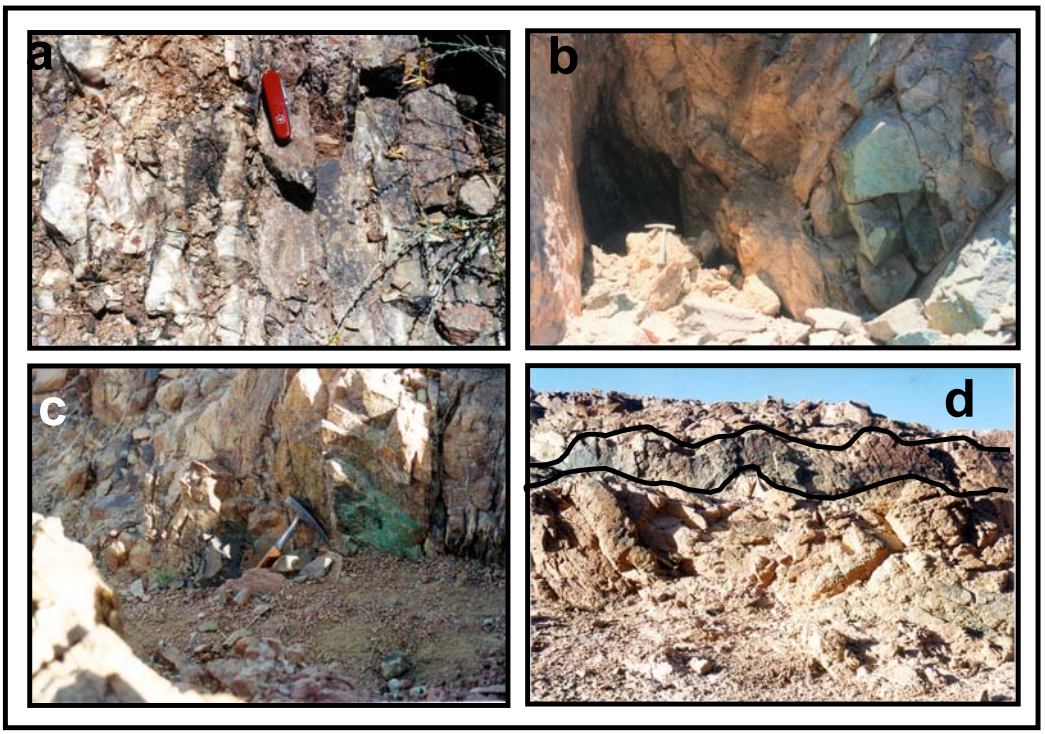

Fig.4. (a)- Silicification in biotite granite showing quartz stockworks at St. Catherine's Monastery area. Looking NE. (b)- Cu- enrichments (malachite) along the younger granite and basic dyke. Looking SW. (c) - Abandoned Cu-mine showing chrysocola enrichment. Looking NE. (d)- Sharp Contact between younger granite and basic dyke showing ferrugination and Cu- enrichments. Looking N30E.

3- Abandoned Copper Mines

Approximately 15 km northeast of Saint Catherine, outside the Saint Catherine ring-dyke complex, is a known copper occurrence (fig.4b). These prospects may date back to Pharonic times. Copper oxide minerals occur along the contacts of a dark-colored, biotite-rich diorite dyke with coarse-grained orthoclase granite it has intruded. This contact is faulted and trends N 40 E, with an apparent strike length of approximately 600 m. The fault zone is several centimeters wide, and is pervasively stained dark red with hematite. Most of the 1 to 2.5 m of clayey material is the product of argillic alteration, as well as hematite-limonite-goethite as a result of supergene processes. Malachite forms a coating on surfaces and occupies the site of altered plagioclase within the dyke rock (Fiig.4c&d). The amount of alteration associated with the original vein is unclear, but was interpreted to be minor. Numerous white and massive quartz veins were observed to be associated within the fault zone. Historic prospecting activity had followed along the strike of the vein, producing 5-10 m pits, where the entire exposure was within the oxidized zone

The lack of significant alteration zones associated with this mineral occurrence, and the limited aerial extent of mineralized rocks in the vicinity indicates that the site contains only sub-economic quantities of copper. The source of mineralization however, is unknown, and the site may merit additional study.

Petrography

Samples were collected approximately 5 km ENE of Saint Catherine village along fracture zones. The variation of rock compositions ranges from rhyolite to microgranite porphyries, quartz monzonite and biotite granite.

Rhyolite to Microgranite Porphyries

The rock varies in size from fine to medium-grained rhyolitic to microgranitic dyke. It is pink in color, porphyritic with an aphanitic groundmass, with 10% milky potassium feldspar phenocrysts (Fiig.5a). Groundmass is approximately half quartz, half potassium feldspar, intergrown, with minor plagioclase and contains 1-2% goethite and hematite as 0.5 – 1.5 mm pseudomorphs after pyrite.
Petrographyically the rock contains 75% groundmass, mainly comprised of fine-grained quartz and potassium feldspar. The mineral composition is made up 35 - 40% quartz, 25 - 40% potassium feldspar (as groundmass and phenocrysts), 5 - 20% plagioclase, 10 - 15% sericite and clays, 2-3% micas (biotite and muscovite), and 1-2% iron oxides.

The rock contains large euhedral to subhedral potassium feldspar crystals (up to 1 cm) that are almost entirely altered to sericite and clay. Albite phenocrysts are 0.5 x 1 mm to 2 x 5 mm, and have altered to sericite and clays while retaining grain shape and twinning. It also contains anhedral quartz grains up to 0.7 mm in diameter, some of which display resorption textures. Biotite crystals up to 1 mm in length were present in the rock and highly altered to sericite, clay, and chlorite. And minor iron oxides as hematite and goethite, 1 mm in diameter, after pyrite.

The groundmass consists primarily of fine-grained crystalline quartz and potassium feldspar intergrown in a granophyric texture. Perthitic textures are abundant and quartz and alkali feldspar form radiate granophyric rims around the edges of larger phenocrysts. A myrmeketic texture is formed with the intergrown of quartz and feldspar which altered to sericite and clay (Fig.5b). Quartz shows weak wavy extinction.

The texture of the rock, especially the presence of resorbed quartz grains in a crystalline matrix suggests a relatively high level intrusion. The rock has been significantly weathered with over half of the potassium feldspar and nearly all of the biotite converted to sericite and clay. The pinkish color of the rock is caused by extremely fine-grained hematite pervasively disseminated within the alteration minerals.

Quartz Monzonite

The rock is porphyritic, phaneritic, pinkish gray with greenish black areas. It contains approximately 70% feldspar, half as phenocrysts (Fig.5c), 15% quartz as fine-grained groundmass, 15% fine-grained biotite, altered to chlorite in patches up to 5 x 8 mm. Petrographycally, the rock contains 33% potassium feldspar phenocrysts, 25% matrix feldspar, 20% quartz, 15% chlorite after biotite, 5% iron oxides (3-4% hematite, 1% magnetite), 1% epidote, 1%interstitial sericite and clays. Large feldspar crystals (up to 7 mm in diameter), dominate the rock. Most are subsequent potassium feldspar, generally pervasively altered to sericite, clay, and minor calcite. Other large feldspar crystals with an elongate habit are interpreted to have been plagioclase prior to pervasive sericitization. Feldspar phenocrysts crystals show a thin rim of generally unaltered plagioclase. Biotite phenocrysts crystals (up to 4 mm in length) are altered to chlorite with interleaved ilmenite and magnetite (Fig.5d).

Groundmass consists of intergrown quartz and potassium feldspar (0.5 mm average in size). Minor granophyric textures are present. Most of the fine-grained potassium feldspar has been altered to sericite and clay. Rare epidote-clinozoisite occurs locally with feldspar. The opaque minerals are made up with disseminated anhedral and fractured magnetite grains up to 0.4 mm in diameter (Fig.5e). Several of the magnetite grains contain minute inclusions of pyrite. Late patches of hematite occur through the rock as very fine grains in the finer-grained potassium feldspar and as clots adjacent to altered mafic minerals.

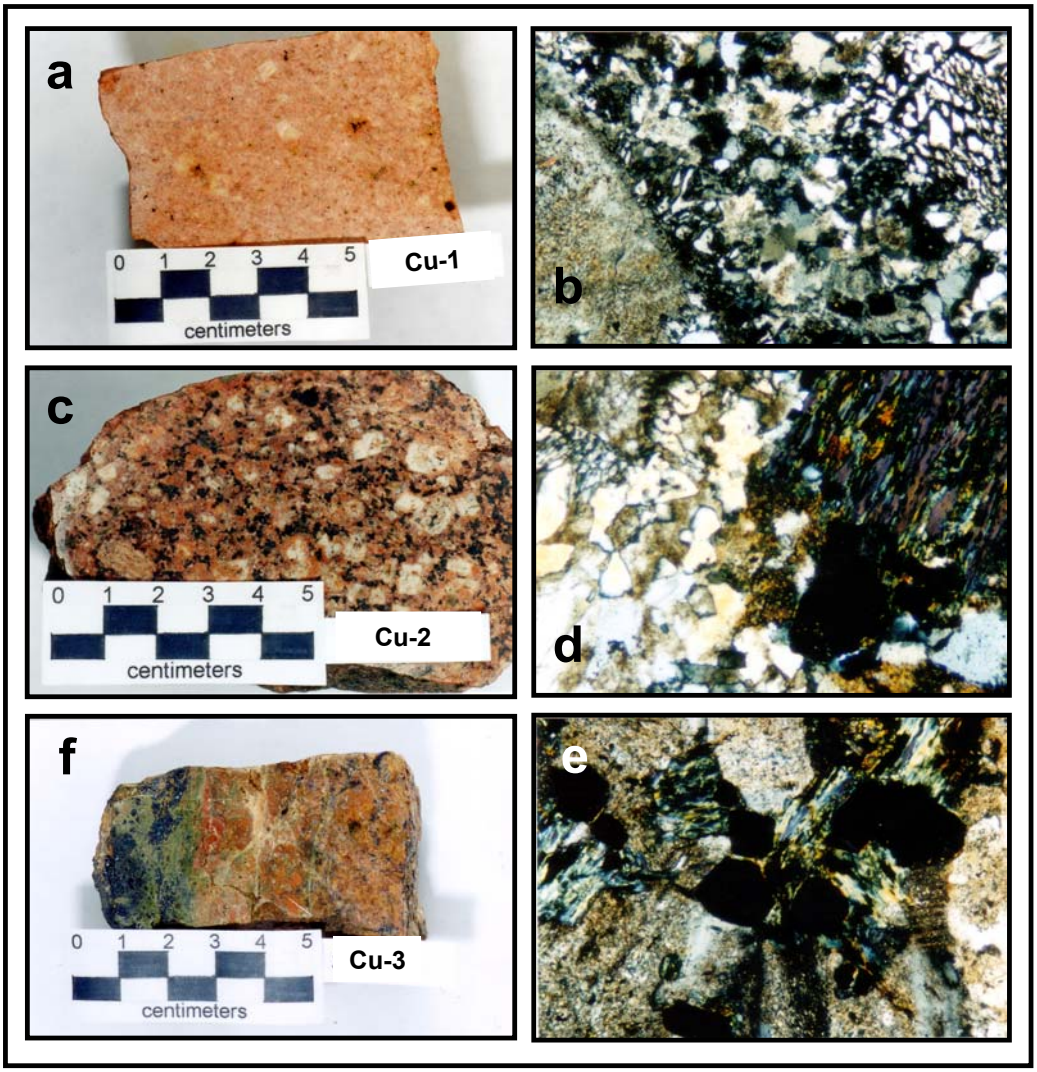

Fig. 5. (a)- Porphyritic rhyolite with K-feldspar phenocrysts (handspecimen). (b)- Myrmekitic texture in microgranite between quartz and K-feldspar. (c)- Porphyritic qz-monzonite with K-feldspar Phenocrysts. (d)- Sericitization associated with chlorite and magnetite in porphyritic qz-monzonite. (e)- Quartz-monzonite showing sericitization in albite with relict albite twinning and associated with magnetite (20X). (f)- Silicified qz-monzonite with epidote-hematite-magnetite-qz-vein.

Rocks that marked by silification are weakly porphyritic and contain light green and black vein of epidote and minor chlorite with hematite and minor magnetite (Fig.5f). Petrographically, the rock contains 35% quartz, 25% potash felspar, 20% albite, 15% sericite/clays, 3% iron oxides, and 2% micas (biotite-muscovite). Perthitic and granophyric textures are observed. Quartz grains exhibit weak undulatory extinction.

Biotite Granite

This rock is phaneritic, porphyritic, pink gray and white, containing 35% 4 – 8 mm rounded white feldspar phenocrysts, 35% pink, angular potassium feldspar grains, 20% biotite 1 – 3 mm in size, 10% quartz (Fig.6a). Petrographically, it contains 35% plagioclase, 20% potassium feldspar, 20% quartz, 10% sericite/clay, 13% chlorite, and 2% magnetite (Fig.6b). Plagiocalse occurs as 3 – 8 mm euhedral to subhedral phenocrysts in a mostly medium-grained, granular matrix of interlocking grains. Potassium feldspar occurs as both phenocrysts and matrix, while quartz is only found as matrix and forms subhedral to anhedral crystals. Feldspars are extensively altered to sericite and clays. Pale green chlorite, has replaced 0.5 – 1.5 mm biotite crystals, and is associated with magnetite. Late muscovite veinlets up to 0.1 mm in width crosscut both feldspars and quartz.

Samples collected from the slope directly east above the Monastery of St. Catherine form 0.5 – 0.6 m wide quartz vein cutting the biotite granite. The rock is light gray to milky white, very fine to medium-grained, with crystalline quartz vein. Minor disseminated sulfide, specular hematite and pyrolusite, which contributes areas of gray color (Figs.6c&d). Minor iron oxides and sericite-epidote alteration is associated with the vein margin in wall rock. Quartz vein in thin section is very fine-grained, well crystalline with later medium-grained open-space-filling crystalline quartz. Opaque minerals are hematite and goethite, possibly after pyrite, and minor pyrolusite.

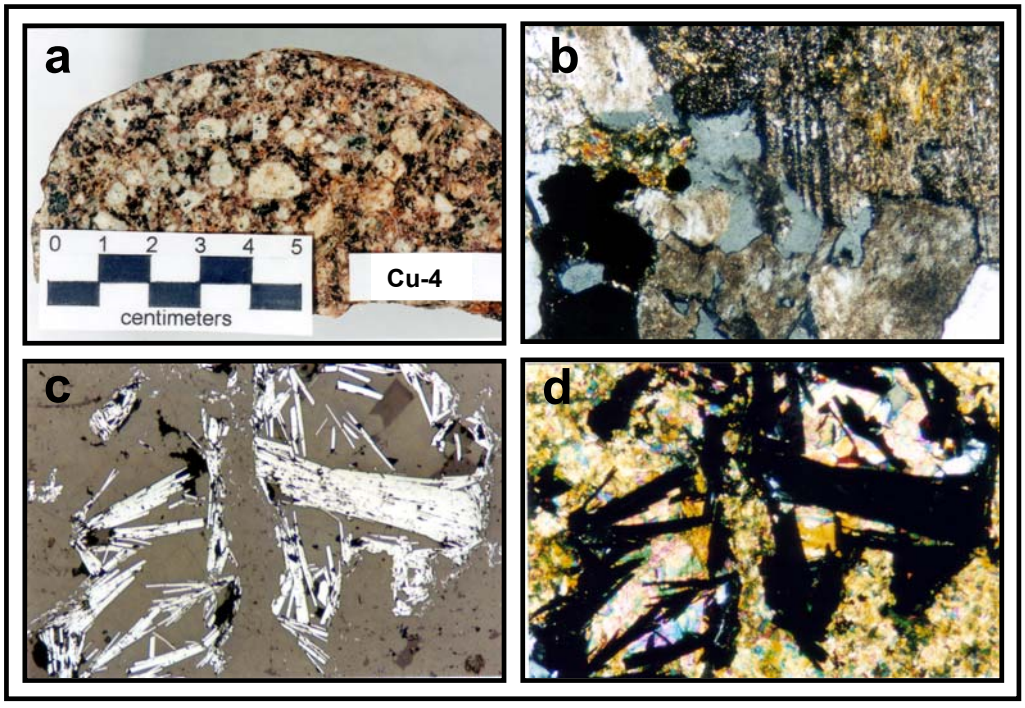

Fig.6.(a)- Porphyritic biotite showing K-feldspar, plagiocalse and biotite as phenocrysts. (b)- Euhedral magnetite grains associated with chlorite sericitic feldspar in biotite granite (20X). (c & d)- Specular hematite crystals in a fine-grained epidote matrix (PPl & XN respectively, 20X).

Environmental impact of copper and heavy metals on human health

The area under investigation is characterized by the presence of sulfides mineralization; supergene enrichments as well as abandoned copper mines. It is important indeed to analyze the importance of environmental impacts on human health for the expected existence metals in the area. This is a first step to predict potential pollution problems that could occur as well as to resolve newly identified contamination problems to minimize the impact on living ecosystem.

Metals are one of the essentials for the development of our society. These metals are also essential for life functions. Copper occurs in Saint Catherine area in natural deposits as ores associated with gangue minerals. Mining activities have a considerable impact on the environment and is only one of the pathways by which metals enter the environment. These activities affect relatively small areas but can have a large local impact on the environment. Release of metals from mining sites occurs primarily through acid mine drainage and erosion of waste dumps and tailings deposits.

The tailings and waste rock deposits close to the mining area are the source of the metals. The type of metal contamination around copper mines mainly depends on the composition of the mined copper ore and the associated gangue minerals. When these deposits contain sulfides in the presence of oxygen which are exposed to the surface, acid mine drainage results. The sulfides could be in the form of pyrite, pyrrhotite and chalcocite minerals. This acid mine drainage will contain high levels of metals. When these leachates reach rivers, a widespread contamination of waters, soils, and vegetation by toxic concentrations of metals and metalloids can occur (Down and Stocks, 1997; Wilmoth et al., 1991). Increased concentrations of Cu, Zn, Pb, Co, Ni, Cd, As and others (> 0.1%) have been reported from several sites with high metal concentrations in soils and plants close to mining activities (Ernst, 1974; Brooks, 1994; Alloway, 1995). Arsenic concentrations in soils and plants affected by mining activities have been frequently reported (Wild, 1975; Porter and Peterson, 1975; De Koe, 1994). Cu, Zn, As and Al concentrations were reported to be concentrated in leaves rather than roots planted close to mining activities (Jaune et al., 1995).

Mines all around the world must obey rules in view of public health; otherwise public health is damaged extremely. These mines must be far away from settlements and underground waters, agriculture, tourist and environment as well as must be operative correctly. Carcinogen heavy metals are associated with valuable metals such as gold, silver, and copper. They found dissolved with them and become mobile and then can pass to underground water, air, plants and environment. Consequently, the end point reached from all kinds of contaminations is human and major concern is human's chronic exposure. In another words, the carcinogen heavy metals passing from the ores to human by water and other ways. Arsenic and mercury are the most dangerous metals among them reaching to human. Many reports had been reported that cancers and chronic diseases resulted from arsenic and mercury. Even if the mine ends or is closed, due to the presence of heavy metals, which are not decomposed and not degraded, mobile, public health problems will continue.

Zinc, chrome, cadmium, lead and nickel were reported in the water, leaf and soils close to the abandoned copper mines (Jaune et al., 1997; Hart and Hines, 1994; Laybauer and Bidone, 1998a). Contamination of aquatic organisms like fish by mercury released in the environment by mining activity has been reported too in various rivers around mining activities (Lindquist et al., 1984; Hacon, 1991).

The safe level of chemicals in drinking water for copper has been set at 1.3 ppm in the drinking water by United States of Environmental Protection Agency (USEPA). USEPA believes this is the maximum contaminant level of protection that would not cause any of the potential health problems. USEPA has found copper to potentially cause health effects when people are exposed to copper at levels above the standard limit. Short periods of exposure can cause gastrointestinal disturbance, such as nausea and vomiting. Use of water that exceeds the safe level over many years could cause liver and kidney damage (USEPA, 1999 and 1994). The same results have been reported by Salem et al., (2000, this volume) in drinking water contaminated with heavy metals especially copper and cadmium.

Copper is widely used in household plumbing materials. It may occur in drinking water either by contamination of the source water or by corrosion of copper water pipes. It is rarely found in source water, but copper mining and smelting operations and municipal incineration may be sources of contamination. Ore extraction, flotation, gravity concentration, acid leaching cementation, and mercury amalgamation are the main metallurgical technologies with environmental impacts.

Saint Catherine area needs to be investigated to construct a geochemical model for contaminants released by acid mine drainage and tailings as well as to delineate these metals in the environment. This environmental protection plan will help to avoid any environmental impacts on settlements and Bedouins in the area.
It is important to keep in mind the risks of health, safety, and hygiene for miners and their families which caused by toxic pollution and the discharging of a significant amount of waste water into superficial and underground waters, contaminating soils, dispersing numerous solid residues, and releasing substantial quantities of heavy metals.

The public and governmental agencies in Egypt are responsible for regulation and control as well as the environmental standards that ensuring the safety for workers and surrounding communities. The government's approach along with the Non-Governmental Organizations (NGO's) should provide education for industrials and public on human health problems, environment protection, environmental management tools, at the same time public should obey rules and cooperate with the government for cleaner environment.

CONCLUSIONS

Field and petrographic investigations suggest that sericitization at wadi Qeisum area could be the result of weak porphyry copper style alteration or a weak hydrothermal event which long postdates magmatism as well as a result of intense weathering. It seems unlikely that any significant economic mineralization was associated with late quartz veins around the Monastery of St. Catherine, given the apparent of sulfide mineral assemblage and hydrothermal textures common in epithermal gold systems. The lack of significant alteration zones associated with the mineral occurrence at the abandoned copper mine, and the limited aerial extent of mineralized rocks in the vicinity indicates that the site contains only sub-economic quantities of copper. A special consideration should be given to the contact between the biotite granite and the biotite diorite dikes for favorable environment for base or precious metals mineralization. It seems likely that the remobilization for base and/or precious metals in this site may have resulted from hydrothermal fluids during the emplacement of the biotite diorite along the biotite granite contact. The source of mineralization however, is unknown, and the area may need further investigation as well as the predicted favorability areas by remote sensing analysis.

Mines must be operative correctly and must obey rules; otherwise public health is damaged extremely. Potential pollution problems arise from mining and tailings activities should be taken into consideration by constructing geochemical model for contaminants released by acid mine drainage and tailings to avoid any pollution problems that have impact on living ecosystems.

Acknowledgements
The authors are grateful for the fruitful discussion with Dr. Murray Hitzman and Alan Lloyd from Colorado School of Mines, Geology Department, Golden, Colorado.

References

Alloway BJ, 1995. Heavy metals in soils, 2nd ed. London: Blackie Academic and Professional, 368p.

Bech J, Poschenrieder C, Llugany M, Barcelo J, Tume P, Tobias F, Barranzuela J, Vasque E, 1995. Arsenic and heavy metal contamination of soil and vegetation around a copper mine in Northern Peru. J. the Science of the Total Environment 203, 83- 91.

Bentor Y.K., 1985. The crustal evolution of the Arabo-Nubian massif with special reference to the Sinai Peninsula. Precambrian Research, 28, p.1-74.

Brooks R.R. 1993. Geobotanical and biogeochemical method for detecting mineralization and pollution from heavy metals in Oceania, Asia and the Americas. In: Markert B,(Eds): Plants as biomonitors. Indicators for heavy metals in the terrestrial environment. Weinheim: VCH, 127-153.

Crippen, R. E., 1988a. The dangers of underestimating the importance of data adjustments in band ratioing, Int. J. Remote Sensing, 9, 767-776.

Down C.G, Stocks J., 1977. Environmental impact of mining. London: Applied Science Publishers, 371p.

El-Fouly A., (1992), Information Extraction and Integration in Mineral Exploration, University of Arizona, Tucson, Arizona.(Unpublished Ph.D. Dissertation) P.219

El-Fouly A., M.Poulton and C.Glass (1992), Hi_res: A Highly Integrated Raster Based Exploration System. IGARSS'92, International Geoscience and Remote Sensing Symposium, Vol.II, pp.935

El-Gawaby, M.A., Helmy, M.E., El-Kaliuby, B.A., Shendy, E.H. 1989. Possibilities for porphyry copper mineralization in South Sinai. Proc. 2nd Conf. Geol. Sinai Develop., Ismailia, p.59-64.

El-Gawaby, M.A. 1984. Image linear analytical approach to copper-mineral exploration in South Sinai, Egypt. International Atomic Agency, United Nations Educational, Scientific and Cultural Organization.

El-Masry, N.N., El-Kaliuby, B.A., Khawasik, S.M., El-Gawaby, M.A. 1992. Reconsideration of the Geologic Evolution of Saint Catherine ring dyke, South Sinai. Proc. 3rd Conf. Geol. Sinai Develop., Ismailia, p.229-238.

Hacon S.P., 1991. Mercury contamination in Brazil, with emphasis on human exposure to mercury in the Amazonian region. WHO/UNEP.

Hart B.T., Hines T., 1994. Trace elements in rivers. In: Salbu B and Steinnes E. (Eds): Trace Elements in Natural Waters. CRC press.

Laybauer L, Bidone E. 1998a. Mass Balance Estimation of Natural and Anthropogenic Heavy Metal Fluxes in Streams Near Camaqua Copper Mines, Rio Grande do Sul, Brazil. In: Environmental Geochemistry in the Tropics, Wasserman J.C, Silva-Filho E.V, Villas-Boas R. (Eds), Berlin: Springer- Verlag, p.127-137.

Lindqvist O., Jernelov A., Johanson K., Rodhe H., 1984. Mercury in the Swedish environment. Global and local sources. Report PM 1816, Natl. Swed. Environ. Prot. Board. Solna.

Salem, H. M., Eweida, E, A., and Farag, A., 2000: Heavy Metals in Drinking Water and their Environmental Impact on Human Health. The International Conference of Environmental Hazards Mitigation, 9-12 Sept., 2000, Cairo University, Egypt, p.542-556 (this volume).

Stern R.J., Gottfried, D. Hedge, C.E., 1984. Late Precambrian rifting and crustal evolution in the Northeastern Desert of Egypt. Geology, v.12, p.168-172.

USEPA, 1994. Drinking water standards and Health Advisories Table. Region IX, 75 Hawthorn Si., San Francisco, California.

USEPA, 1999. Drinking water and Health. EPA816-k-99-001.

Wilmoth R.C., Hubbard S., Burckle, J.O., Martin J.F. 1991. Production and processing of metals: their disposal and future risks. In: Merian E, (Eds): Metals and their compounds in the environment. Occurrence, analysis and biological relevance. Weinheim: VCH, 19-65.